Ordering and the nature of the spin flop phase transition in $MnPS_3$

2000 J. Phys.: Condens. Matter 12 1845

(http://iopscience.iop.org/0953-8984/12/8/327)

J. Phys.: Condens. Matter **12** (2000) 1845–1854. Printed in the UK PII: S0953-8984(00)05982-8

Ordering and the nature of the spin flop phase transition in $MnPS_3$

D J Goossens†§, A R Wildes‡, C Ritter‡ and T J Hicks†

† Department of Physics, Monash University, Clayton 3168, Australia

‡ Institut Laue–Langevin, 6 rue Jules Horowitz, BP 156, 38042 Grenoble Cédex 9, France

E-mail: goossens@rsc.anu.edu.au

Received 13 July 1999, in final form 21 December 1999

Abstract. Powder diffraction patterns were measured on a high quality sample of manganese thiophosphate, $MnPS_3$, at temperatures between 2 and 120 K and magnetic fields between 0 and 60 kOe. In zero field, the magnetic moments in $MnPS_3$ are collinear and normal to the ab planes. On applying a sufficiently large magnetic field along the normal to the ab plane, it was found that the moments flop towards the b axis, in agreement with a dipole–dipole interaction model for the anisotropy. The width of this transition was found to be greater than 20 kOe. No evidence for critical fluctuations was seen during the spin flop phase transition.

1. Introduction

Manganese thiophosphate, $MnPS_3$, is a layered, quasi-two-dimensional (2D) Heisenberg antiferromagnet. The magnetism is due to the manganese ions, Mn^{2+}, which lie in the ab planes. $MnPS_3$ has a small anisotropy which aligns the moments collinear with the perpendicular to the ab layer planes, hereafter defined as the z direction (figure 1). The Néel temperature, T_N, is 78 K at low fields ($H_z < 40$ kOe, where H_z is applied in the z direction) [1]. $MnPS_3$ has a monoclinic structure with space group $C2/m$. Lattice parameters are $a = 6.077$ Å, $b = 10.524$ Å, $c = 6.796$ Å and $\beta = 107.35^\circ$ [2]. Hence, the c axis is not quite parallel to the z direction. In the layers, the manganese atoms form a honeycomb lattice. Each manganese is neighboured by three manganese atoms and three P_2 pairs [2]. Each such layer lies between a pair of sulphur layers. These triple structures are joined to each other by Van der Waals forces between adjacent sulphur layers. The distance between manganese layers and the complex exchange path give rise to the 2D magnetism exhibited by $MnPS_3$.

Each Mn^{2+} ion interacts antiferromagnetically with its three intraplanar nearest neighbours, and is ordered ferromagnetically compared with its interplanar nearest neighbours [1]. The exchange interactions have been measured by inelastic neutron scattering to be $J_1 = -0.77 \pm 0.09$ meV, $J_2 = -0.07 \pm 0.03$ meV, $J_3 = -0.18 \pm 0.01$ meV and $J' = 0.0019 \pm 0.0002$ meV, where J_i is the exchange interaction between ith nearest neighbours within the Mn plane and J' is the interaction between first interplanar neighbours [3].

At 5 K, $MnPS_3$ undergoes a spin flop phase transition [4, 5] when magnetic field of $H_{sf} = 47$ kOe is applied along the z direction. The width of the transition is in excess of

§ Corresponding author. Present address: Research School of Chemistry, Australian National University, Canberra 0200, Australia.

0953-8984/00/081845+10$30.00

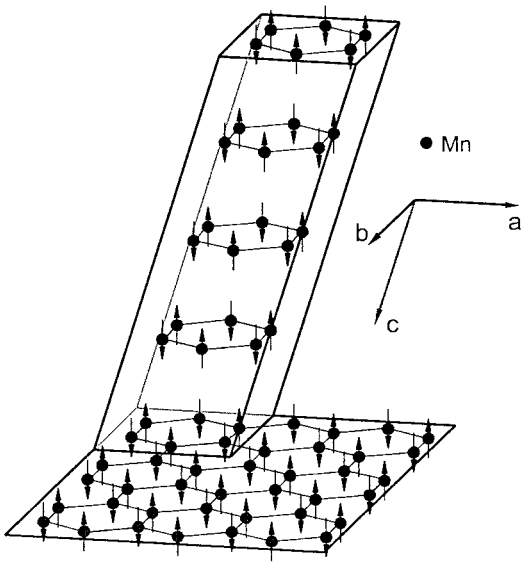

Figure 1. The low-field spin structure of $MnPS_3$. The spins point along the z direction which lies perpendicular to the ab plane.

20 kOe, so fields greater than 60 kOe are required to make the spins point along a direction entirely within the layer planes. The spin structure of the spin flop state is not known, although the spins probably lie in the ab planes. This can be visualized with reference to figure 1.

The nature of the spin flop phase transition in 2D antiferromagnets with Heisenberg spins and small Ising-like anisotropies has been discussed by, amongst others, Landau and Binder [6], de Groot and de Jongh [7], Cowley *et al* [8] and Pich and Schwabl [9, 10]. Except for [10], all this work has focused on square lattice systems, making a study of the honeycomb structured $MnPS_3$ a useful check on the established theories of phase transitions and universality.

Landau and Binder [6] suggest that the phase transition consists either of two closely spaced second order phase transitions or a single first order phase transition. However, the spin Hamiltonian used to parametrize the uniaxial anisotropy is an anisotropy in the exchange interaction, which is unlikely to be the real physical mechanism. As the nature of the phase transition will depend heavily on the symmetry of the anisotropy, this is important. Further, the choice of Hamiltonian means that at applied fields greater than the spin flop field, H_{sf}, the system moves into the universality class of the XY model, where it exists in a Kosterlitz–Thouless bound vortex state [11], and does not show true long range order (LRO).

The Mermin–Wagner theorem [12] states rigorously that a purely Heisenberg 2D spin system cannot enter a LRO state at non-zero temperatures. The work of Pich and Schwabl is based on the suggestion that the dipolar interaction is sufficient to break the symmetry and bring about the ordering. As this interaction will be present in any array of magnetic moments, it must be considered in $MnPS_3$.

The intention of this work is to determine the nature of the magnetic ordering in $MnPS_3$ through the spin flop, and hence gain insight into the spin flop phase transition. In particular, the low coordination and monoclinic symmetry of $MnPS_3$ offers the possibility of unusual and highly interesting behaviour, which could result in a good test of the validity of general theories of ordering and universality.

2. Experimental details

Experiments were conducted on the D2B powder diffractometer at the ILL. The sample consisted of hundreds of platelet-like crystals stacked inside a vanadium cylinder. The sample mass was 1.44 g. Diffraction patterns were collected at applied fields of up to 60 kOe and temperatures between 2 and 120 K.

A vapour transport method was used to grow a large number of crystals [2]. When grown, the samples appear as platelets of approximate dimensions $8 \times 8 \times 0.1$ mm^3. The z direction is the direction normal to these platelets. Small discs were cut from these samples and stacked inside a cylindrical vanadium sample holder to make a composite sample. The holder was filled with a helium atmosphere to minimize background. The composite sample was therefore an attempt to create a sample with random directions of a and b but a unique direction of z.

The sample was placed in a 60 kOe vertical cryomagnet, with the common z axis aligned vertically. The field direction was therefore collinear with the moment directions, as required for a spin flop transition. This configuration had the added advantage that in zero field the moments were all perpendicular to the scattering plane, and therefore the Bragg peaks showed the maximum magnetic Bragg intensity. The sample could not be rotated inside the 60 kOe cryomagnet, so no averaging across orientations could be done. Further, it is possible that only a few crystals might have contributed to each reflection. Hence, the intensity of a given reflection could successfully be mapped out as a function of field or temperature, but the ratio of the intensity of one reflection to another could not be expected to obey the structure factor. This means that a Rietveld analysis was not possible. The variability in sample alignment over the course of the experiment was monitored by using peaks with a magnetic structure factor of zero (see equation (1), below). The intensities of these peaks were found to be stable over time, indicating that the sample did not move or change orientation to a significant degree. This also had important ramifications for the magnetic structure as a function of field, which will be discussed in section 4. The large crystal sizes gave rise to the possibility of extinction, but agreement with the known model at low field and temperature allowed the conclusion that extinction was unlikely to be important.

3. Results versus temperature

Due to the honeycomb lattice, there are crystallographically two types of manganese site in $MnPS_3$. Therefore the magnetic and nuclear unit cells are of the same size and the magnetic and nuclear Bragg peaks coincide. The magnetic structure factor is [1, 13]

$$F_M \approx \mu_\perp 4\mathrm{i} \sin\left(\frac{2\pi k}{3}\right) \tag{1}$$

where k is a Miller index and $\mu_\perp$ is the component of the magnetic moment perpendicular to the scattering vector. Therefore Bragg peaks for which $k = 3n$ (where n is an integer) have zero magnetic intensity. Throughout this work, the high temperature nuclear intensity of each peak was used to calibrate its magnetic intensity. This result could be verified at low temperature and zero applied magnetic field by relating the measured intensity to the total intensity predicted by the nuclear and magnetic structure factors combined, as the magnetic structure is known under these conditions [1]. Hence, nuclear intensities were found at low and high temperatures, and were found to agree.

Figure 2 shows diffraction patterns measured at 2 K, 80 K and 120 K in zero applied field. Most of the intensity is provided by peaks of the form $hk0$, because scattering in which $l \neq 0$

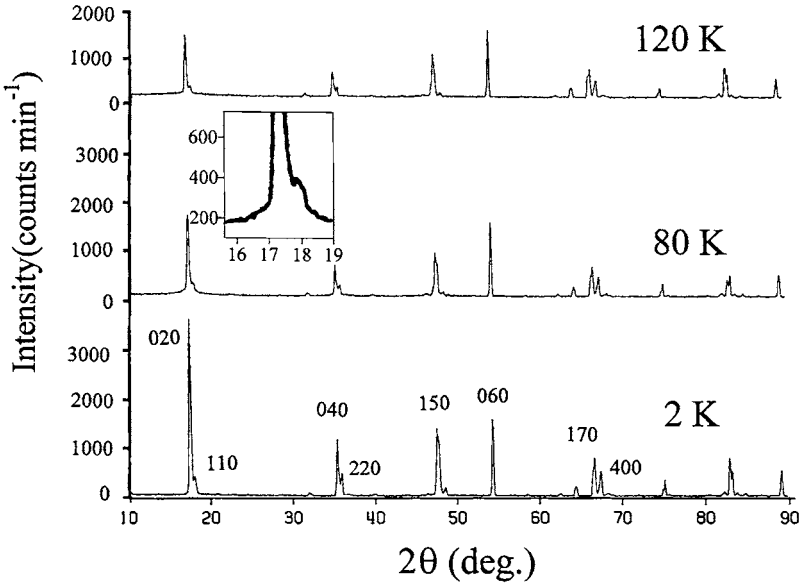

Figure 2. Diffraction patterns of compound sample of $MnPS_3$ at 2, 80 and 120 K in zero field. The inset shows diffuse scattering around the base of 020 and 110 peaks at 80 K.

must have some component perpendicular to the a^*b^* plane. The a^*b^* plane is *not* coplanar with the ab plane, but is inclined to it at an angle of approximately 18° because the c axis is not perpendicular to the ab plane. The large vertical acceptance angle of the detectors on D2B means that this does not affect data collection on the $hk0$ peaks, but it does mean that peaks for which $l \neq 0$ are present. This provides extra data when solving for the magnetic structure.

The diffraction patterns collected at temperatures close to T_N showed diffuse scattering peaks centred around the antiferromagnetic Bragg peaks. This scattering had previously been attributed to a second true 2D phase in this material [13], but this has subsequently been shown to be 2D critical scattering [14]. The patterns collected at 80 and 120 K show these features, with the diffuse scattering broader at 120 K as the correlation lengths become shorter. Peaks for which $k = 3n$ show no variation in intensity with temperature, indicating no magnetic component and verifying equation (1). The Bragg intensity of the magnetic peaks decreases until it is close to zero at 80 K, as expected.

Data were collected as a function of temperature in an applied field of 55 kOe. At this field, the sample is in the SF phase for temperatures below 35 K and in the zero field antiferromagnetic phase at temperatures above 35 K and below T_N [5]. Magnetic intensity as a function of temperature for the 020 Bragg peak was found to increase to a maximum at 60 K before falling to zero near 80 K. Thus, the maximum intensity is reached in the AF phase. The scattering vector for this reflection is parallel to the b axis. Thus, the moments are pointing more in the direction of the b axis in the SF phase than they are when in the AF phase. The conclusion is that moments do not flop into the direction of the a axis.

The diffraction patterns collected in the SF phase showed no new Bragg peaks, suggesting that the magnetic unit cell is unchanged by the spin flop; the magnetic periodicities are maintained. This aids in modelling the data and solving the spin flop spin structure.

4. Results versus field

Figure 3 shows a number of diffraction patterns collected in various applied fields at a temperature of 2 K. Comparison with figure 2 shows an absence of diffuse scattering centred around the antiferromagnetic Bragg peaks, a conclusion which is verified by subtracting the patterns. This indicates that there are no fluctuations in the moments, so the transition is not a phase transition in which the spins exhibit critical fluctuations. Hence, it is probably a continuous rotation of spins from one state to another. These results agree with Pich and Schwabl [9, 10].

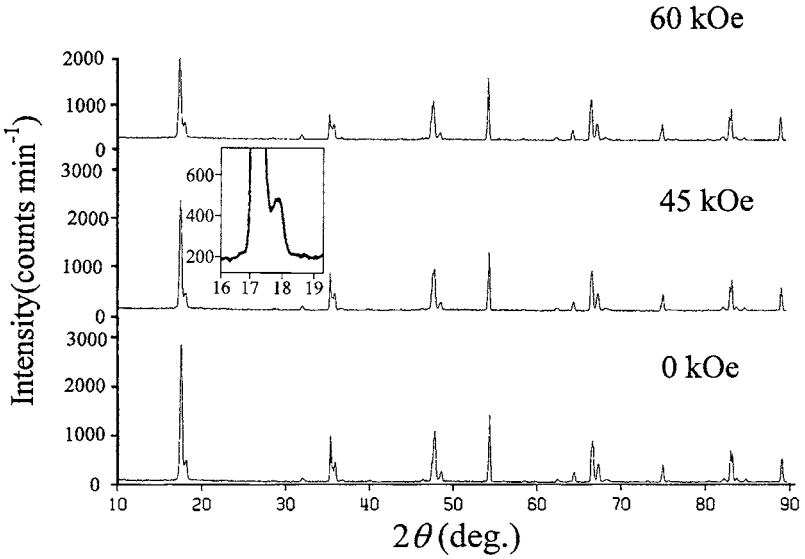

Figure 3. Diffraction patterns in 0, 45 and 60 kOe at 2 K. The inset shows lack of diffuse scattering around the base of 020 and 110 peaks at 45 kOe.

Figure 4 shows the integrated magnetic intensities of a number of Bragg peaks as functions of field at 2 K. No peak loses all of its magnetic intensity, indicating that for each peak there is always some component of the moment perpendicular to the scattering vector. No peak for which $k = 3n$ shows a dependence on intensity on applied field, meaning that equation (1) holds at all fields and any canted state must have this structure factor.

To extract the spin structure as a function of field from these data, each spin in the unit cell was assigned two angles; an angle with respect to the z direction and an angle with respect to the a direction, denoted ϕ and θ respectively, and defined in figure 5. There are four atoms in the unit cell, and so this gives eight parameters. However, equation (1) arises only if the moments pair up such that the moments in each pair are antiparallel. Hence it is necessary to fit four parameters—a ϕ and θ for each pair of moments. The structure can be thought of as a four sublattice antiferromagnet in which pairs of sublattices are antiparallel. It is assumed that the magnitude of the moment is unaffected by the spin flop. This should be reasonable given that the temperature and the magnetic coordination are unchanged by the spin flop phase transition.

Using least squares fitting, ϕ and θ were determined for each pair of sublattices at each applied field. This model with non-collinear spins found that the spins tipped away from the z direction as field increased, such that at 60 kOe $\phi = 67^\circ \pm 9^\circ$ and $65^\circ < \theta < 115^\circ$ for all atoms at all fields. However, statistical reliability in fitting procedures requires that there be

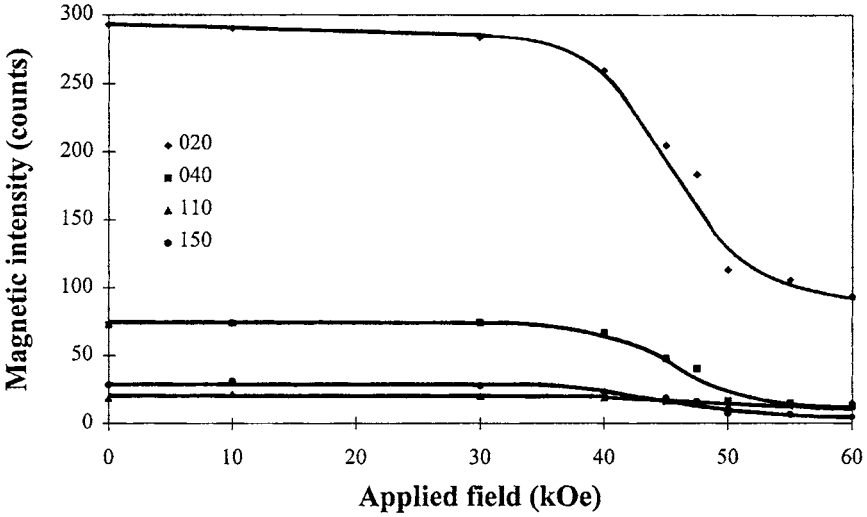

Figure 4. Integrated magnetic intensity of a number of Bragg peaks as a function of field at 2 K. Data are plotted as points and fits as lines.

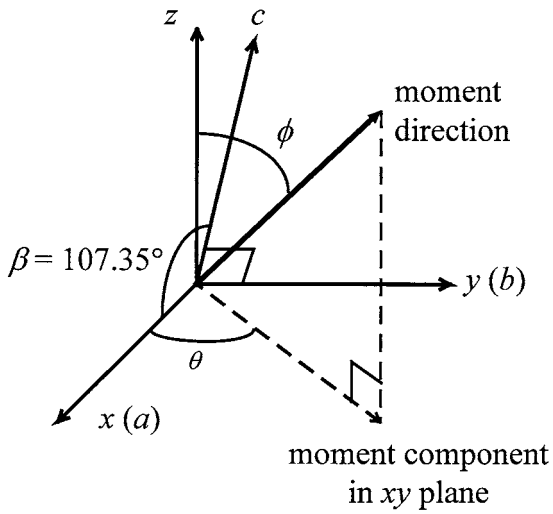

Figure 5. Definition of angles and directions.

three times as many data points as fitted parameters. While more than 12 magnetic peaks can be brought into the fit, many of these have relatively low intensity, and so large errors. The large uncertainty in the data from these small peaks led to large uncertainties in the results of the fit using the non-collinear model. Consequently similar but simpler models were applied to see if the fit results could be improved.

A second model was tried in which it was assumed that the spin structure remained collinear. This model had only two free parameters, namely ϕ and θ for the whole spin lattice. Results showed that the spins tip away from the z direction such that $\phi = 85^\circ \pm 5^\circ$ and $\theta = 68^\circ \pm 8^\circ$ at 60 kOe. This result and that from the non-collinear structure suggest spins pointing more along b than a. This is to be expected, as figure 4 shows large reductions in the

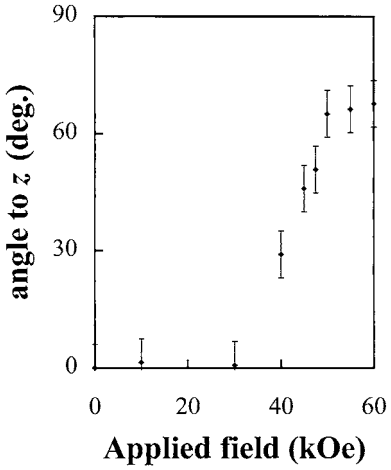

Figure 6. Angle of collinear spin structure to the z direction, if restricted to the bz plane, as a function of field at 2 K.

magnetic intensity of the 020 and 040 reflections as field increases, indicating that the moments become closer to being parallel with the b direction as the spin flop takes place.

The dipole–dipole interaction energy was calculated for a collinear structure by summing over $41 \times 41 \times 41$ unit cells. The calculation was based on the fundamental expression for the energy, U, of one dipole in the field of another [15]

$$U = \frac{\boldsymbol{m}_1 \cdot \boldsymbol{m}_2}{r^3} - \frac{3(\boldsymbol{m}_1 \cdot \boldsymbol{r})(\boldsymbol{m}_2 \cdot \boldsymbol{r})}{r^5} \tag{2}$$

where $\boldsymbol{m}_1$ and $\boldsymbol{m}_2$ are the magnetic moment vectors and $\boldsymbol{r}$ is the vector connecting them. The calculation showed that if the spins are restricted to the ab plane, then pointing along the b axis minimizes their energy. It is very important to sum across all three spatial dimensions, due to the monoclinic structure of $MnPS_3$. Pich and Schwabl [9] suggest that in some substances a 2D summation is sufficient; this is found not to be the case in $MnPS_3$.

On the basis of this dipolar interaction result, a third model was tried, a 'restricted collinear' model, in which the spin direction was restricted to the bz plane ($\theta = 90^\circ$). Hence there was only one free parameter, ϕ. This model again found that the spins tipped away from the z direction and gave $\phi = 67^\circ \pm 3^\circ$ at 60 kOe. Figure 4 shows the fitted magnetic intensity for this model plotted as a line. The other models gave almost identical results and are not plotted. This phase transition can be pictured by referring to figure 1 and simply placing a spin pointing along the positive b direction in place of each up spin and a spin pointing along the negative b direction in place of each down spin. This is because the magnetic correlations remain the same, but the spins are rotated.

Table 1 compares the observed and calculated magnetic intensities for the most significant magnetic reflections of the form $hk0$ at fields of 0 and 60 kOe at 2 K. It shows that, apart from the 110 reflection which suffered considerable unreliability due to overlap with the 020 and low intensity, the very simple model works well for all the significant reflections for which the magnetic form factor of the Mn^{2+} is significant.

The question arises as to which model is nearest to the physical reality. To answer this, magnetometry results can be used. An estimate of the angle the spin makes to the z direction at 60 kOe and 2 K, based on the difference between the 'parallel' susceptibility at 4.5 K and 60 kOe and the true perpendicular susceptibility at 4.5 K from SQUID measurements is $70^\circ \pm 5^\circ$

Table 1. The fraction of the total scattering due to the magnetic structure in the low field antiferromagnetic phase and in the high field spin flop phase from experiment and from the restricted collinear model, in which the spins were restricted to the bz plane. F_M gives the magnetic structure factor and F_N the nuclear. The 110 reflection suffers from low intensity and overlap with the 020. The 170 and 080 show magnetic intensity within error of zero in the spin flop phase due to the magnetic form factor of Mn^{2+}. All peaks for which $k = 3n$ show zero magnetic intensity in both phases experimentally and also in the calculations.

		$F_M^2/(F_M^2 + F_N^2)$			
		$T = 2$ K $H = 0$ kOe		$T = 2$ K $H = 60$ kOe	
2θ	Reflection	Calculated	Observed	Calculated	Observed
17.448	020	0.65	0.65	0.22	0.21
18.233	110	0.67	0.72	0.35	0.56
35.318	040	0.59	0.60	0.17	0.13
47.644	150	0.42	0.43	0.10	0.09
48.613	240	0.44	0.41	0.13	0.10
66.576	170	0.22	0.24	0	0
74.702	080	0.11	0.15	0	0

[5]. This is in excellent agreement with the results from the restricted collinear model and the non-collinear model. Statistical tests show that the extra three parameters in the non-collinear model do not improve the fit sufficiently to be significant. Hence, the conclusion is that the collinear model, with the spins restricted to the bz plane, is the most appropriate. When a similar restriction was placed on the non-collinear model, the two values of ϕ proved to be the same as the single ϕ value from the restricted collinear fit.

Figure 6 shows the angle ϕ as a function of field for the collinear structure in which $\theta = 90^\circ$. The points at high fields show very weak field dependence, but as the errors on the points are about 5°, the actual slope possesses considerable uncertainty. The weak dependence can be seen to be quite reasonable by reference to figure 7.

Figure 7 shows moment versus applied field data collected using a SQUID magnetometer on $MnPS_3$ at 5 K, plotted as solid circles. The field has been applied along the z direction. Other field directions gave no spin flop and have not been shown. The field derivative is plotted as open circles. Because the gradient does not reach a constant value even at 70 kOe, this shows that the spin flop progresses quite slowly above 47 kOe, making the small gradient at the high field end of figure 6 reasonable. It is suggested that the H_{sf} measured by the SQUID is physically meaningful as the field at which the spins are rotating most rapidly from the AF to the SF state.

The lack of diffuse scattering in figure 3 suggests that the spin flop phase is not a Kosterlitz–Thouless phase, as this is a state with strong short range order which should give rise to diffuse scattering. It is reasonable that this is the case and that the magnetic structure is collinear given that the monoclinic symmetry of the system results in a dipolar interaction which is not cylindrically symmetrical about the z direction. This lack of symmetry results in a single preferred spin orientation, which prevents a non-collinear or a Kosterlitz–Thouless phase from forming. It should be noted that this result is contingent upon calculating the dipole field due to the 3D array of moments. If a single plane is used, the field at a site will have a symmetry which is not representative of the 3D system.

In their work on the spin dynamics of a 2D honeycomb lattice with dipolar anisotropy, Pich and Schwabl [9, 10] have predicted the effect of an external field on the ground state of $MnPS_3$. They predict that the spin orientation of the Mn^{2+} will cease to be collinear with the

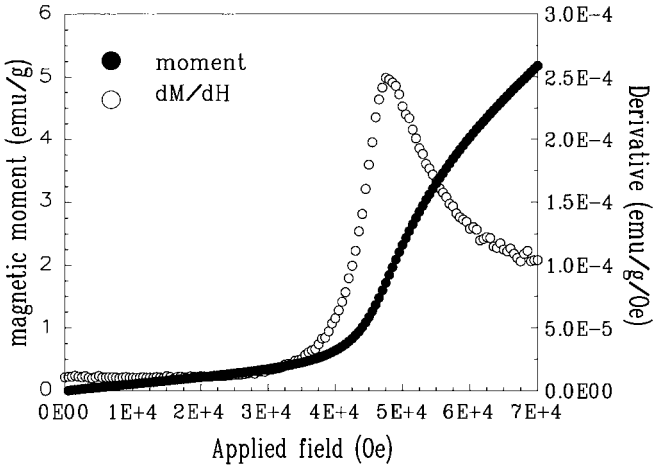

Figure 7. Magnetic moment versus field measured at 5 K on a SQUID magnetometer with the magnetic field along the z direction.

normal to the ab planes at a critical field of

$$H_0^c = \frac{E_0}{g\mu_B} \tag{3}$$

where E_0 is the gap in the spin-wave dispersion at the Brillouin zone centre. A 'canted' ground state is then stable, where the spins will rotate continuously with increasing field until they will lie in the ab planes (the 'flop' orientation) at a second field

$$H_0^{sf} = H_0^c\left(\frac{2|J_1|z + A_0^{xx} - \overline{A}_0^{xx} - A_0^{zz} - \overline{A}_0^{zz}}{2|J_1|z - A_0^{xx} - \overline{A}_0^{xx} + A_0^{zz} - \overline{A}_0^{zz}}\right) \tag{4}$$

where A_0^{ii} are the Fourier transforms of the dipole tensor on one sublattice and $\overline{A}_0^{ii}$ are the Fourier transforms of the interaction between the two sublattices. The spin-wave gap has been measured to be $E_0 = 0.499$ meV [3], and the same authors have used the equations of Pich and Schwabl to calculate the magnitude of $(g\mu_B)^2 = 0.0534$ meV Å^3. Substituting these values into the equations above the first critical field is calculated to be $H_0^c = 86.2$ kOe, much larger than the measured 45 kOe, and the second at $H_0^{sf} = 86.3$ kOe; thus, the field width of the canted phase is much smaller than the measured 20 kOe.

The calculations of Pich and Schwabl are for a 2D system for which $MnPS_3$ is only an approximation. The value above of $(g\mu_B)^2$ was calculated for a 2D lattice and is a factor of 4 smaller than expected which is strange in a magnetic system with no spin–orbit coupling. If a value of $(g\mu_B)^2 = 4 \times 0.0534 = 0.2136$ meV Å^3 is used in the above calculation the first critical field is found to be $H_0^c = 43.1$ kOe and the second at $H_0^{sf} = 43.3$ kOe. While the first critical field is approximately the same as that found experimentally, the second field is much smaller. The discrepancies both in the values of $(g\mu_B)^2$ and the magnitudes of the critical fields may be accounted for if the interlayer coupling is considered in the theory. The interlayer dipolar interaction may also have some effect.

It appears, however, that qualitatively the picture of Pich and Schwabl is correct and the spin flop transition consists in fact of three phases.

5. Conclusions

The nature of the magnetic order and the phase transitions in $MnPS_3$ has been explored using neutron diffraction. The magnetic intensity of the Bragg peaks was found to be zero at temperatures above 80 K. Diffuse scattering was observed beneath the magnetic Bragg peaks at temperatures close to and considerably above the phase transition temperature. This indicated that the order/disorder phase transition is a critical phase transition. No such diffuse scattering was observed during the spin flop phase transition, indicating that the spins do not undergo critical fluctuations. It appears to be a continuous rotation of the spins from the z to the b direction, with the 'spin flop field' measured by a magnetometer being the field at which the rotation is most rapid.

The results of Pich and Schwabl [9, 10] were found to be qualitatively correct, in that the spin flop transition appears to be governed by the dipolar interaction. A collinear canted phase was observed during the transition, but evidence for a non-collinear phase is weak. The collinearity may be explained by the lack of cylindrical symmetry in the dipolar interaction.

Acknowledgments

We would like to thank Alan Holland and Peter Cross for their technical assistance. DJG is pleased to acknowledge the financial assistance of the Australian Institute of Nuclear Science and Engineering and the Australian Nuclear Science and Technology Organization. This work is supported by the Australian Research Council.

References

[1] Kurosawa K, Saito S and Tamaguchi Y 1983 *J. Phys. Soc. Japan* **52** 3919–26
[2] Ouvrard G, Brec R and Rouxel J 1985 *Mater. Res. Bull.* **20** 1181–9
[3] Wildes A R, Roessli B, Lebech B and Godfrey K W 1998 *J. Phys.: Condens. Matter* **10** 6417–28
[4] Okuda K, Kurosawa K, Saito S, Honda M, Yu Z and Date M 1986 *J. Phys. Soc. Japan* **55** 4456–63
[5] Goossens D J and Hicks T J 1998 *J. Phys.: Condens. Matter* **10** 7643–52
[6] Landau D P and Binder K 1981 *Phys. Rev.* B **24** 1391–403
[7] de Groot H J M and de Jongh L J 1986 *Physica* B **141** 1–36
[8] Cowley R A, Aharony A, Birgeneau R J, Pelcovits R A, Shirane G and Thurston T R 1993 *Z. Phys.* B **93** 5–19
[9] Pich C and Schwabl F 1994 *Phys. Rev.* B **49** 413–16
[10] Pich C and Schwabl F 1995 *J. Magn. Magn. Mater.* **148** 30–1
[11] Kosterlitz J M and Thouless D 1973 *J. Phys. C: Solid State Phys.* **6** 1181–203
[12] Mermin N D and Wagner H 1966 *Phys. Rev. Lett.* **17** 1133–6
[13] Wildes A R, Kennedy S J and Hicks T J 1994 *J. Phys.: Condens. Matter* **6** L335–41
[14] Wildes A R, Harris M J and Godfrey K W 1998 *J. Magn. Magn. Mater.* **177–181** 143–4
[15] Scott W T 1962 *The Physics of Electricity and Magnetism* (New York: Wiley) p 373